Kelemen, P.B., Kikawa, E., and Miller, D.J. (Eds.)
Proceedings of the Ocean Drilling Program, Scientific Results Volume 209

3. Sulfide Mineralization at Site 1268, Mid-Atlantic Ridge, Ocean Drilling Program Leg 209[1]

D. Jay Miller[2]

ABSTRACT

This paper presents sulfide mineral occurrence, abundance, and composition in samples from hydrothermally altered peridotite and gabbro recovered during Ocean Drilling Program (ODP) Leg 209 from south of the 15°20′N Fracture Zone on the Mid-Atlantic Ridge at Site 1268. Most of the sulfide minerals occur in veins and halos around veins in serpentinized peridotite. The only sulfide phases reported that occur in proximity to gabbro are those associated with a mafic intrusion into serpentinized peridotite. Sulfide mineral species change predictably downsection but are perturbed coincident with a breccia interpreted to be generated by intrusion of a gabbroic magma. The general downhole trend suggests sulfide mineral precipitation in conditions with decreasing sulfur and oxygen fugacity. Sulfide minerals that indicate precipitation at relatively higher sulfur and oxygen fugacity occur in the central core of the intrusion breccia. Sphalerite makes a fleeting appearance in the sulfide mineral assemblage in samples from the lower part of the intrusion breccia. Strongly contrasting pyrite compositions suggest at least two episodes of pyrite precipitation, but there is no clear morphological distinction between phases. Heazelwoodite, tentatively identified in shipboard examinations, could not be confirmed in this study.

INTRODUCTION

Leg 209 was the first Ocean Drilling Program (ODP) expedition designed to investigate spatial (and potentially temporal) heterogeneities

[1] Miller, D.J., 2007. Sulfide mineralization at Site 1268, Mid-Atlantic Ridge, Ocean Drilling Program Leg 209. *In* Kelemen, P.B., Kikawa, E., and Miller, D.J. (Eds.), *Proc. ODP, Sci. Results,* 209: College Station, TX (Ocean Drilling Program), 1–18. doi:10.2973/odp.proc.sr.209.004.2007
[2] Integrated Ocean Drilling Program, Texas A&M University, 1000 Discovery Drive, College Station TX 77845-9547, USA.
miller@iodp.tamu.edu

Initial receipt: 25 January 2007
Acceptance: 20 April 2007
Web publication: 25 June 2007
Ms 209SR-004

in Earth's mantle. The location (north and south of the 15°20′N Fracture Zone on the Mid-Atlantic Ridge; Fig. F1) was selected because precruise dredging and submersible surveys had revealed extensive exposures of mantle peridotite along the walls of the rift valley and on off-axis topographic domes. Four of the eight sites occupied during Leg 209 recovered substantial volumes of rock exhumed from Earth's mantle and emplaced on the western wall of the rift valley. These four sites (1268, 1271, 1272, and 1274) sampled mantle peridotite emplaced in different sections of the ridge-transform system from the inside corner high to near the ridge segment center, as well as a site between the segment center and end.

F1. Mid-Atlantic Ridge bathymetry, p. 7.

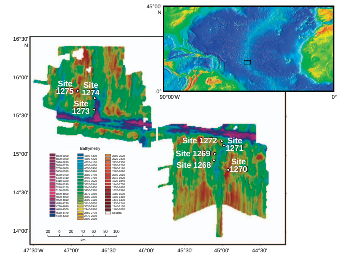

One of the many striking discoveries from Leg 209 was the degree of variability in hydrothermal alteration of serpentinized peridotites. In general these ranged from alteration of olivine to serpentine accompanied by alteration of orthopyroxene to tremolite and talc to complete replacement of serpentinized peridotite with talc. A distinct manifestation of the variability in alteration of the serpentinized peridotites recovered during Leg 209 is the abundance and distribution of sulfide mineralization. This study forms part of a collaborative effort among several shipboard scientists to document and interpret serpentinization reactions in and hydrothermal alteration of Earth's mantle and to test theoretical and experimental models of fluid circulation in the oceanic crust. This report characterizes the chemical variability of sulfide mineralization in samples from Hole 1268A.

PREVIOUS ODP WORK

Two ODP expeditions were sailed prior to Leg 209 with the objective of sampling exposures of Earth's mantle from fast- and slow-spreading ridges. Leg 147 to Hess Deep (Shipboard Scientific Party, 1993) cored six holes from 10 to 94 meters below seafloor (mbsf). Four of these holes are separated by <20 m; the other two are located ~250 and ~400 m away from the four-hole location. Only two of the holes penetrated deeper than 40 mbsf, and total recovery from all six holes was ~65 m. From this suite of samples, Puchelt et al. (1996) determined that the sulfide mineralogy was dominated by Ni-bearing phases and that the presence of native metals and Ni-Fe alloys indicated mobilization of sulfur under strongly reducing conditions. They also estimated the primary sulfur content of the mantle section represented by the samples to be ~300 ppm. Prichard et al. (1996) demonstrated that the partially serpentinized rocks retain platinum-group elements.

During Leg 153 to the Kane Fracture Zone area on the Mid-Atlantic Ridge (MARK), two holes were cored (to 126 and 200 mbsf) within meters of each other but with nearly 150 m of recovery (Shipboard Scientific Party, 1995). Gaggero et al. (1997) report a primary sulfide mineral assemblage from the MARK samples of pentlandite, chalcopyrite, and pyrrhotite, with a secondary sulfide mineral assemblage of violarite and mackinawite.

SITE 1268

Whereas serpentinized peridotites recovered during the previous two ODP expeditions targeting exposures of mantle rock were from closely spaced drilling targets, during Leg 209 we sampled four sites (1268, 1271, 1272, and 1274) from the western wall of the Mid-Atlantic Ridge separated by nearly a degree of latitude and from both north and south of the 15°20′N Fracture Zone. The cores from these sites represent 600 m of penetration and show an extensive range in degree and style of hydrothermal alteration and sulfide mineralization. Owing to the division of labor among shipboard scientists, this study focuses only on recovery from Site 1268.

Twenty-nine cores were recovered to a depth of nearly 148 mbsf. Two general types of lithologies were recovered at Site 1268, ultramafic (harzburgite and dunite) and gabbroic rocks. The upper 100 m of the section is nearly exclusively ultramafic except for a 15-m interval between 63 and 77 mbsf that includes a gabbroic intrusion breccia. Most of the sulfide minerals described in this paper were found in veins and in halos around veins in serpentinized peridotite. The only sulfide phases noted that occurred in association with mafic rocks are those from cores within or in close proximity to the mafic intrusion breccia (Cores 209-1268A-12R through 15R). Below 100 mbsf, the recovery was predominantly gabbroic rock. Details of the lithologic variability are available in the Leg 209 *Initial Reports* volume (Shipboard Scientific Party, 2004).

Cores from this site are intensely veined with fairly abundant but highly localized sulfide and sulfide/oxide-bearing veins. Sulfide mineral bearing veins compose as much as 10% of the total vein volume and at least 1 vol% of the bulk core. Primary sulfides were identified on board as pyrrhotite and pentlandite and the presence of millerite was identified as an alteration product, suggesting reducing conditions during mobilization of sulfur.

METHODS

Mineral identifications were made from examination of 98 polished thin sections. Quantitative analyses of sulfide minerals were performed using a Cameca Camebax SX50 electron microprobe in the Department of Geology and Geophysics at Texas A&M University. Operating conditions were 15 kV with a beam current of 30 nA, a counting time of 30 s, and a 1-µm focused beam. Natural sulfide standards from Chuck Taylor (FeS_2, ZnS, PbS, GaAs, and Sb_2Te_3) were used for calibration of Fe, S, Zn, Pb, As, and Sb, respectively, and routinely analyzed as unknowns to check for drift. Pure Cu wire (also analyzed as a drift standard), Ni, Co, and Au were used as calibration standards.

RESULTS AND DISCUSSION

Sixty-one thin sections from the shipboard suite were examined for sulfide mineral presence and abundance, and an additional 37 thin sections were prepared from sulfide-bearing core samples from Site 1268. The results of petrographic examination of sulfide and oxide abundance are presented in Table T1. Sixteen samples with the most abundant and petrographically diverse sulfide mineral assemblages were selected for detailed mineral chemistry analysis. The electron microprobe analyses of sulfide minerals are presented in Table T2.

There is a distinct change in sulfide mineral abundance, morphology, and speciation downsection. The sulfide mineral suite present in these samples is shown in Figure F2, and the change in assemblage expected

T1. Sulfide mineral occurrences, p. 11.

T2. Compositions of sulfide phases, p. 13.

F2. Sulfide phases, p. 8.

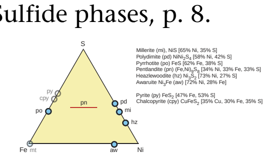

with decreasing oxygen and sulfur fugacity is shown in Figure F3. The uppermost samples from Hole 1268A contain millerite as lenses, blebs, and needles in pyrite. The pyrite contains Ni and Co for the most part in roughly equal proportions (<1–2 wt% each), although a single analysis has much more Co than Ni. Within samples from the second core taken starting at 15 mbsf, the assemblage includes chalcopyrite and the abundance of millerite decreases markedly, although millerite persists through Core 209-1268A-3R (~23 mbsf).

F3. Expected phase distribution, p. 9.

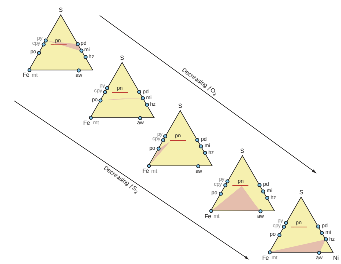

By Core 209-1268A-4R at ~25 mbsf, millerite and chalcopyrite are no longer present, but pyrrhotite is fairly common. Pyrite is still present, but it is found most commonly in disseminations and along late veins that crosscut all other structures. Core 209-1268A-9R, from 49 mbsf, contains the shallowest samples containing analyzed grains of Co-bearing pentlandite. The assemblage of magnetite, pentlandite, and pyrrhotite suggests sulfide mineral precipitation in lower oxygen and sulfur fugacity than the sulfide mineral assemblage in samples from shallower parts of the hole.

Section 209-1268A-12R-3 shows a distinct change in sulfide minerals. Millerite and chalcopyrite rejoin the sulfide mineral assemblage, and pyrrhotite and pentlandite were not detected. The higher sulfur and oxygen fugacity assemblage persists through Core 209-1268A-13R. This interval from Core 209-1268A-12R thorough 14R was identified by the shipboard scientific party as a breccia induced by intrusion of mafic magma. Curiously, although the intrusion breccia extends from the top of Core 209-1268A-12R to the bottom of Core 14R (~63–77 mbsf), the assemblage of millerite/chalcopyrite/±polydymite occurs only between Sections 209-1268A-12R-3 and 13R-1 (66.7–71.1 mbsf). Below this interval, the sulfide minerals rapidly return to the low-sulfur and -oxygen fugacity assemblage (predominantly pyrrhotite and pentlandite) and remain so through the deepest interval sampled. Most of the gabbroic rocks sampled below 100 mbsf did not contain any significant sulfide mineral abundance in the thin sections examined. Sphalerite was also present in three samples from the lower part of the gabbroic intrusion breccia (Sections 209-1268A-14R-3 and 15R-2 and 15R-3). In the lower part of the section, there are two chemically distinct pyrite compositions. One contains as much as 10 wt% Co, the other a few weight percent of Ni with no Co. There is no clear morphological difference between the occurrences of these phases; both occur as disseminated blebs and in veins. Inasmuch as pyrite is commonly indicative of a sulfur and oxygen richer environment, these phases are likely to be late-stage additions to the sulfide mineral assemblage.

SUMMARY

The sulfide mineral assemblage in cores from Hole 1268A changes downsection, potentially reflecting changes in sulfur and/or oxygen fugacity as fluid migrates through the section. Figure F4 illustrates the changes in the sulfide assemblage downsection compared to total sulfide mineral vein fraction and lithology. The sulfide assemblage that suggests precipitation at relatively high sulfur and oxygen fugacities (polydymite and millerite) yields downsection to progressively lower sulfur and oxygen fugacity assemblages (millerite + pyrrhotite, pyrrhotite + pentlandite, and eventually only pentlandite). This series is interrupted by the reappearance of millerite and polydymite coincident with a breccia interpreted to represent the remnants of a gabbroic intrusion,

F4. Hole 1268A lithologies, p. 10.

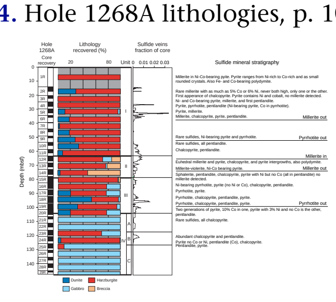

suggesting a coincident increase in sulfur and oxygen during the precipitation of sulfide minerals in this interval. Sphalerite also appears in the mineral assemblage only in the lowermost part of the intrusion breccia. Below the intrusion breccia, the sulfide mineral assemblage is dominated by pentlandite. Even lower sulfur and oxygen fugacity assemblages (pentlandite + awaruite and awaruite + heazelwoodite) tentatively identified during shipboard analysis were not detected in these samples.

ACKNOWLEDGMENTS

This research used samples and/or data provided by the Ocean Drilling Program (ODP). ODP is sponsored by the U.S. National Science Foundation (NSF) and participating countries under management of Joint Oceanographic Institutions (JOI), Inc. Funding for this research was provided by the U.S. Science Support Program (USSSP). I thank Eiichi Kikawa and Ron Frost for helpful reviews.

REFERENCES

Gaggero, L., Cortesogno, L., and Gazzotti, M., 1997. Data report: oxides, sulfides, and associated phases in veins and hydrothermally altered peridotitic rocks. *In* Karson, J.A., Cannat, M., Miller, D.J., and Elthon, D. (Eds.), *Proc. ODP, Sci. Results,* 153: College Station, TX (Ocean Drilling Program), 523–529. **doi:10.2973/odp.proc.sr.153.034.1997**

Prichard, H.M., Puchelt, H., Eckhardt, J.-D., and Fisher, P.C., 1996. Platinum-group-element concentrations in mafic and ultramafic lithologies drilled from Hess Deep. *In* Mével, C., Gillis, K.M., Allan, J.F., and Meyer, P.S. (Eds.), *Proc. ODP, Sci. Results,* 147: College Station, TX (Ocean Drilling Program), 77–90. **doi:10.2973/odp.proc.sr.147.004.1996**

Puchelt, H., Prichard, H.M., Berner, Z., and Maynard, J., 1996. Sulfide mineralogy, sulfur content, and sulfur isotope composition of mafic and ultramafic rocks from Leg 147. *In* Mével, C., Gillis, K.M., Allan, J.F., and Meyer, P.S. (Eds.), *Proc. ODP, Sci. Results,* 147: College Station, TX (Ocean Drilling Program), 91–101. **doi:10.2973/odp.proc.sr.147.005.1996**

Shipboard Scientific Party, 1993. Site 895. *In* Gillis, K., Mével, C, Allan, J., et al., *Proc. ODP, Init. Repts.,* 147: College Station, TX (Ocean Drilling Program), 109–159. **doi:10.2973/odp.proc.ir.147.104.1993**

Shipboard Scientific Party, 1995. Site 920. *In* Cannat, M., Karson, J.A., Miller, D.J., et al., *Proc. ODP, Init. Repts.,* 153: College Station, TX (Ocean Drilling Program), 45–119. **doi:10.2973/odp.proc.ir.153.102.1995**

Shipboard Scientific Party, 2004. Site 1268. *In* Kelemen, P.B., Kikawa, E., Miller, D.J., et al., *Proc. ODP, Init. Repts.,* 209: College Station, TX (Ocean Drilling Program), 1–171. **doi:10.2973/odp.proc.ir.209.103.2004**

Figure F1. Mid-Atlantic Ridge bathymetry (base image from **www.ngdc.noaa.gov/mgg/image/2minrelief.html**) with inset noting location of lower map of Leg 209 drill sites from Shipboard Scientific Party, 2004. Only samples from the southernmost site on the western wall of the Mid-Atlantic Ridge (Site 1268) are discussed in this paper.

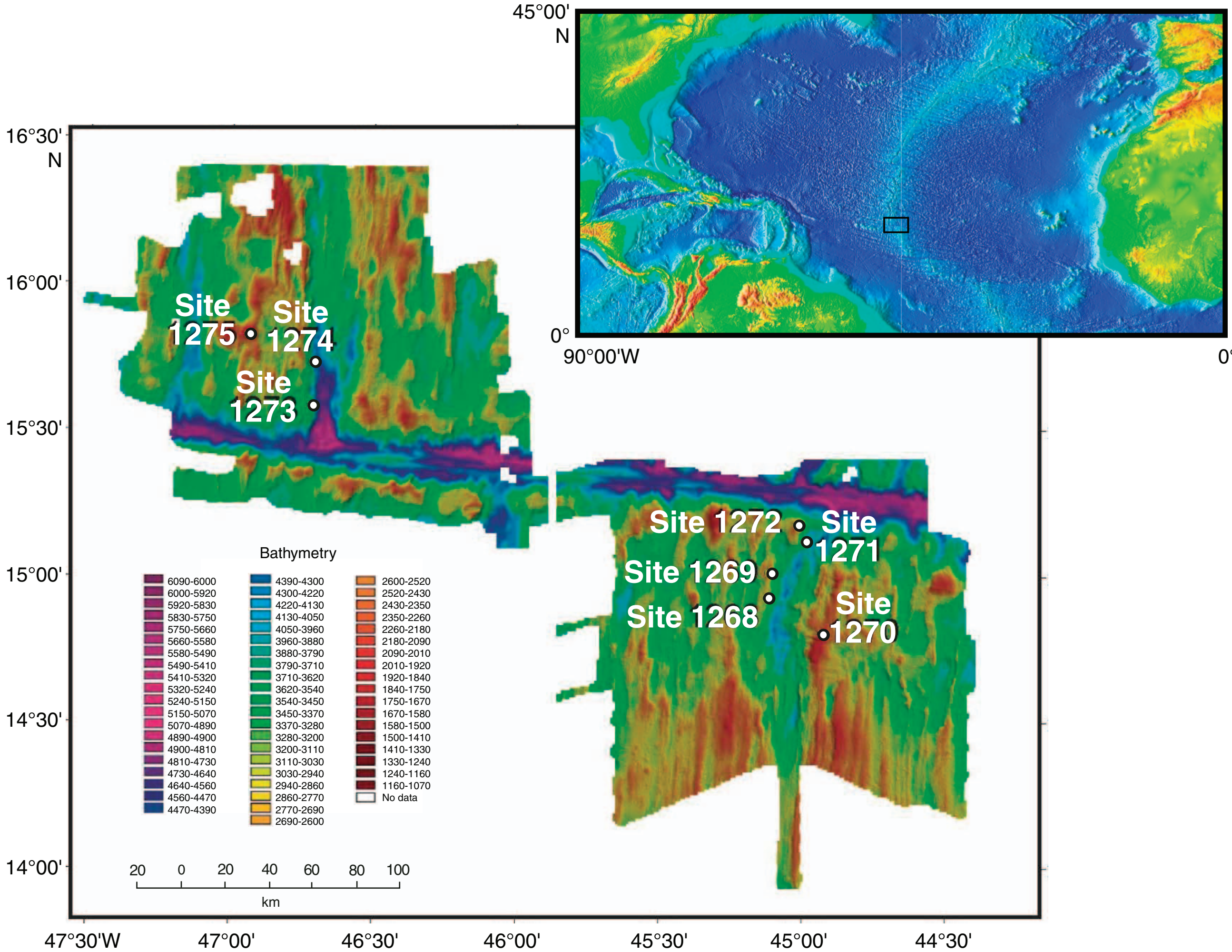

Figure F2. Sulfide phases studying the Fe-Ni-S system. Phases in light gray type occur in samples from Site 1268 but are not part of this system. Chalcopyrite is projected from Cu, magnetite is projected from oxygen, and pyrite is commonly a late phase. mt = magnetite.

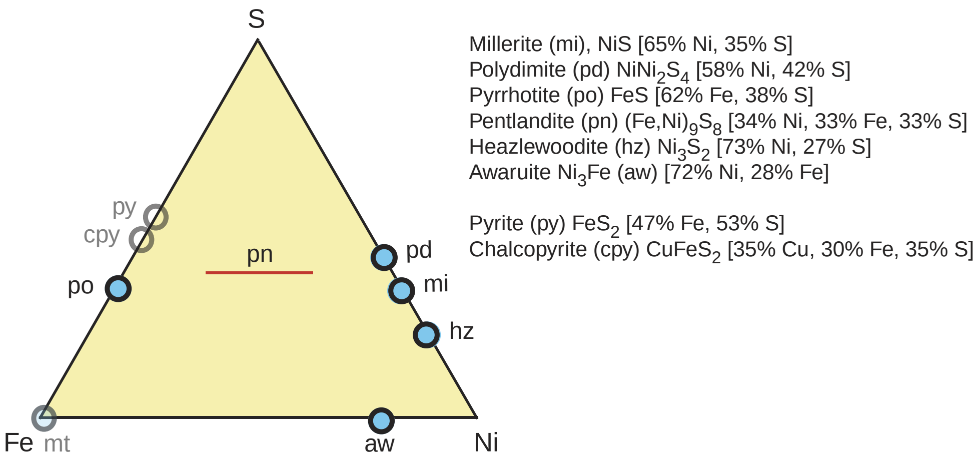

Figure F3. Changes in expected phase distribution with decreasing sulfur and oxygen fugacity. The expected assemblages changes are polydymite (pd) + millerite (mi), millerite + pyrrhotite (po), pyrrhotite + pentlandite (pn), pentlandite + magnetite (mt), magnetite + awaruite (aw), and awaruite + heazelwoodite (hz). py = pyite, cpy = chalcopyrite.

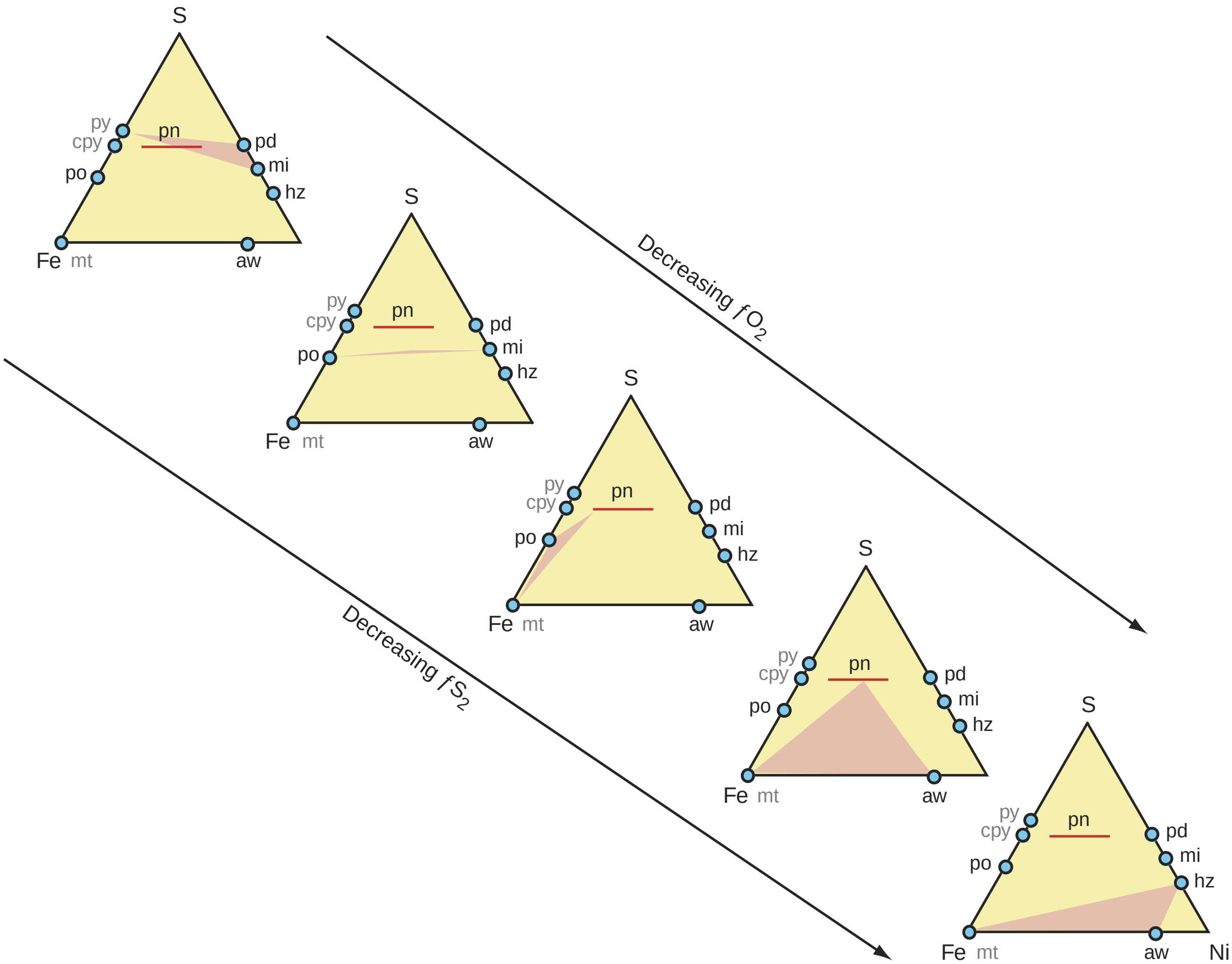

Figure F4. Hole 1268A lithologies, shown as percentages of total recovery for each core (left panel). Total recovery is represented by the black boxes at the far left. Lithologic units are defined in the Leg 209 *Initial Reports* volume (Shipboard Scientific Party, 2004). Dunite was originally >90% olivine; harzburgite includes all ultramafic rocks exclusive of dunite; gabbroic rocks include gabbronorites, microgabbros, and gabbroic rocks of undeterminable mineralogy; and intrusion breccias are mixtures of highly altered, probably originally gabbroic material and ultramafic host. TD = total depth. Right panel is the total fraction of the core accounted for by sulfide veins. Text indicates depths of sulfide phase first and last occurrence.

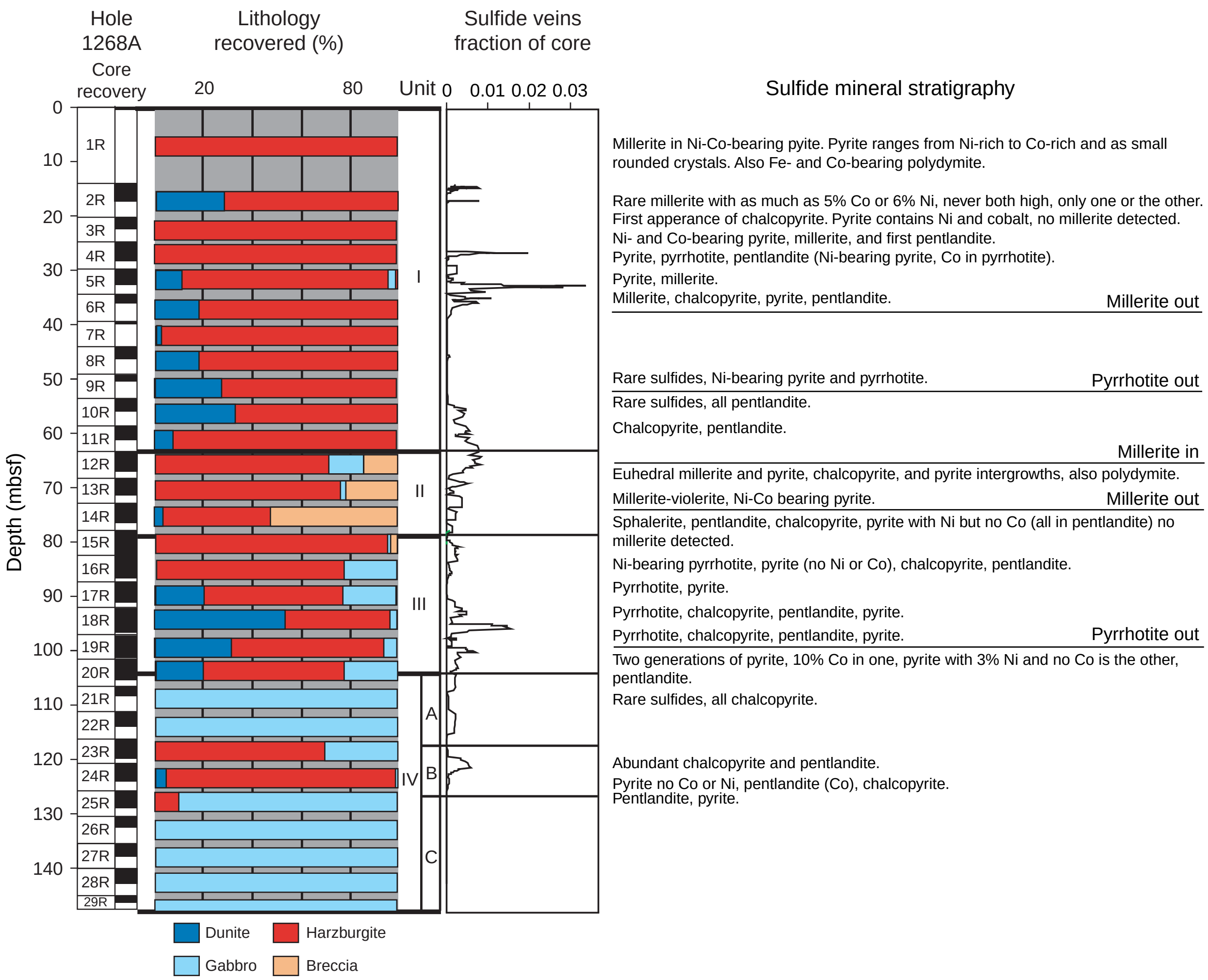

Table T1. Sulfide mineral occurrences in samples from Hole 1268A. (See table notes. Continued on next page.)

Core, section, piece, interval (cm)	Depth (mbsf)	py	cpy	mi	vi	pd	po	pn	sph	hem	mag	sp	
209-1268A-													
1R-1 (9, 53–55)	0.5	**		**		**				t	1		
2R-1 (6, 25–28)	14.3	****		*						t	3		
2R-1 (7B, 44–46)	14.4	t								t	t		
2R-1 (22, 125–128)	15.3	t									t		
2R-2 (4C, 40–43)	15.8	t								t	t		
2R-2 (7, 58–60)	16.0	***	***	*						t	1		
2R-2 (8, 70–73)	16.1	t								t	t	t	
2R-3 (4, 11–13)	16.9	t									t		
3R-1 (3, 8–10)	20.3	**		*	*						t		
3R-2 (1, 7–10)	21.7										2	1	
3R-2 (20A, 109–112)	22.7	t									1		
3R-3 (2, 6–9)	23.2										1	2	
3R-3 (3, 14–16)	23.3	**			*					t	1		
4R-1 (5A, 12–15)	24.9	t								t	t		
4R-1 (20A, 124–127)	26.0	t									t		
4R-2 (9, 57–60)	26.9	**					*				t		
5R-2 (14, 58–61)	31.9	t									t	1	
5R-2 (17, 71–73)	32.0	t										1	
5R-2 (26A, 122–124)	32.5	t									t	1	
6R-1 (10, 58–61)	35.0	t										1	
6R-1 (14, 75–77)	30.6	*					*				1		
6R-1 (15, 106–108)	35.5	t									t		
6R-1 (17, 119–122)	35.6	t										t	
7R-1 (9, 34–37)	39.7	t									t	1	
7R-1 (10, 41–44)	39.8										1	1	
8R-1 (22, 92–95)	44.9						*				1	t	
8R-1 (28, 117–119)	45.2	t					*				t		
8R-2 (4, 23–25)	45.7	**					**				t		
9R-1 (4, 14–16)	49.2							*			t		
10R-1 (16A, 85–88)	54.5											1	
10R-2 (1, 8–10)	55.1	t									t	t	
10R-2 (14, 82–85)	55.9	t									t		
11R-1 (7, 34–37)	58.9							**			1		
11R-2 (4, 17–20)	60.2	t						**		t	t	1	
11R-2 (17, 90–92)	60.9	t						*			t		
12R-1 (2B, 16–18)	63.4	t									t		
12R-1 (3, 47–49)	63.7	*								1	1	1	
12R-1 (6, 74–76)	63.9												
12R-1 (12, 116–119)	64.4	*									t	t	
12R-1 (14, 125–127)	64.5	t								t	t		
12R-2 (7, 35–37)	65.1	1									1	1	
12R-2 (17, 93–98)	65.6	1								t	t	1	
12R-3 (1B, 18–21)	66.3	**						*		t	1		
12R-3 (7A, 63–65)	66.7	**	*	*		*						1	
12R-3 (7, 71–74)	66.8	t										2	
13R-1 (6A, 33–35)	68.5	t									t	2	
13R-1 (6B, 40–43)	68.6	**	*	*								1	
13R-1 (6B, 68–71)	68.9	**	*									t	
13R-2 (1, 3–6)	69.6	t									t	1	
13R-2 (7, 42–45)	70.0	t											
13R-2 (15, 92–95)	70.5	t									t	1	
13R-3 (3, 8–11)	71.1	**		*	*					t	1	t	
14R-1 (7A, 34–36)	73.1	**	*					*	*	t	t	t	
14R-2 (16, 130–133)	75.6	t									t	t	
14R-3 (1, 3–5)	75.8											1	
15R-1 (10, 75–77)	78.6	t								t	t		
15R-2 (6, 66–69)	79.9		*					*	*		t		
15R-3 (1, 15–17)	80.6		*					*	*		t		
15R-3 (5, 135–137)	81.8	t									t	t	
16R-1 (3A, 21–24)	82.6	t									t	1	
16R-2 (1, 31–34)	83.9	t									t	t	
16R-2 (1, 37–40)	84.0	t						t			t	t	
16R-3 (10, 107–110)	86.2												Gabbro
16R-4 (1, 3–9)	86.6												Gabbro
17R-1 (9A, 100–103)	88.4	t						t			t		
17R-2 (7B, 47–49)	89.4	**	**										
17R-2 (15, 100–103)	89.9	*	*					*			t	t	

Table T1 (continued).

Core, section, piece, interval (cm)	Depth (mbsf)	py	cpy	mi	vi	pd	po	pn	sph	hem	mag	sp	
17R-3 (6, 66–68)	91.0										3	1	
18R-1 (4, 61–63)	92.6												
18R-2 (4, 62–65)	93.9	t									t	t	
18R-2 (11A, 118–121)	94.5	t									t	t	
18R-3 (1A, 5–7)	94.6	*									1	t	
18R-4 (11, 88–91)	96.8	***		*				**			t		
19R-1 (2A, 16–18)	97.2										1	1	
19R-1 (2B, 51–53)	97.5	t									1	1	
19R-2 (2, 34–36)	98.7	**											
19R-3 (1, 3–6)	99.9	t									t	t	
19R-3 (3, 19–22)	100.0	t						t			t	t	
20R-1 (2, 8–12)	101.7	*						*			t	t	
20R-1 (8, 96–99)	102.6	1									1		
20R-2 (2, 74–77)	103.8	*	*					*			1	1	
20R-3 (13, 83–85)	105.3		*								t	t	
21R-1 (3, 37–39)	107.0												Gabbro
21R-1 (15, 129–131)	107.9												Gabbro
21R-2 (5, 18–21)	108.3												Gabbro
22R-1 (15, 117–120)	112.4												Gabbro
23R-1 (4C, 57–60)	116.8												Gabbro
23R-1 (8, 126–128)	117.5												Gabbro
23R-2 (3, 18–21)	117.8	t										t	
23R-2 (9, 71–73)	118.4	t					*	*				t	
23R-3 (1, 6–8)	119.0		**					*				t	
24R-1 (10, 78–80)	121.6	**	*					*				t	
24R-2 (9, 101–103)	123.1	t					*	**				t	
24R-2 (14, 129–132)	123.3	t										t	
26R-2 (2, 18–20)	132.1												Gabbro
27R-1 (5B, 64–66)	136.1												Gabbro
28R-2 (1B, 26–28)	141.7												Gabbro
29R-1 (14, 118–120)	146.3										t		Gabbro

Notes: * = relative abundance of sulfide phases in each sample. t = trace, py = pyrite, cpy = chalcopyrite, mi = millerite, vi = violarite, pd = polydymite, po = pyrrhotite, pn = pentlandite, sph = sphalerite, hem = hematite, mag = magnetite, sp = spinel. Numbers are in visually estimated modal percent.

Table T2. Compositions of sulfide phases in selected samples from Hole 1268A. (Continued on next five pages.)

Hole, core, section, piece, interval (cm)	Depth (mbsf)	S	Fe	Co	Ni	Cu	Zn	Total
209-1268A-								
1R-1 (9, 53–55)	0.5	53.4	46.0	0.2	0.3	0.0	0.0	99.9
		53.5	46.5	0.0	0.0	0.0	0.0	100.1
		35.5	1.4	0.2	63.5	0.0	0.0	100.6
		42.1	11.5	3.5	42.5	0.0	0.0	99.5
		35.6	1.5	0.2	61.6	0.0	0.0	98.9
		52.9	42.1	2.3	2.3	0.0	0.0	99.7
		42.1	10.2	4.1	41.9	0.0	0.0	98.4
		42.3	10.9	3.3	43.1	0.0	0.0	99.7
		37.1	3.1	1.7	57.8	0.0	0.0	99.8
		35.5	1.3	0.5	62.4	0.0	0.0	99.6
		42.2	10.7	4.5	41.8	0.0	0.0	99.2
		35.6	0.9	0.1	63.7	0.0	0.0	100.4
		42.0	10.8	4.0	42.1	0.0	0.1	98.9
		52.9	42.5	4.1	0.5	0.0	0.0	100.0
		35.6	1.8	0.3	62.8	0.0	0.1	100.6
		40.4	7.8	3.8	47.8	0.0	0.0	99.8
		35.5	1.9	0.2	63.1	0.0	0.0	100.6
		42.5	10.5	6.0	41.7	0.0	0.0	100.6
2R-1 (6, 25–28)	14.3	52.5	41.3	5.4	0.3	0.0	0.0	99.6
		52.6	42.8	2.7	1.0	0.0	0.0	99.0
		34.7	3.2	0.0	62.4	0.0	0.0	100.4
		53.2	42.5	0.1	2.9	0.0	0.0	98.7
		52.9	44.9	0.0	1.6	0.0	0.0	99.4
		52.6	45.8	0.0	0.1	0.0	0.0	98.6
		53.4	44.6	0.0	1.4	0.0	0.0	99.3
		52.5	45.7	0.1	0.1	0.0	0.0	98.4
		53.3	43.6	0.0	2.5	0.0	0.0	99.3
		53.3	46.6	0.0	0.0	0.0	0.0	100.0
		53.3	44.6	0.2	1.2	0.0	0.0	99.3
		52.4	45.5	0.2	0.5	0.0	0.0	98.6
		52.8	43.9	0.0	1.5	0.0	0.0	98.2
		52.9	46.1	0.0	0.1	0.0	0.0	99.1
		53.3	42.8	0.0	3.5	0.0	0.0	99.6
		52.7	45.9	0.0	0.2	0.0	0.0	98.9
		51.4	42.3	0.0	2.8	0.0	0.0	96.6
		53.0	44.0	0.1	2.4	0.0	0.0	99.5
		52.6	39.8	0.0	6.7	0.0	0.0	99.2
		50.7	45.6	0.0	1.6	0.0	0.0	98.0
		52.3	44.6	0.0	1.6	0.0	0.0	98.5
		53.4	43.9	0.0	2.1	0.0	0.0	99.3
2R-2 (7, 58–60)	16.0	53.2	39.0	0.4	7.7	0.0	0.0	100.3
		53.1	43.7	2.0	1.6	0.0	0.0	100.4
		53.0	42.6	0.5	4.1	0.0	0.0	100.2
		53.0	43.0	0.7	3.5	0.0	0.0	100.2
		52.9	41.9	4.1	1.2	0.0	0.0	100.2
		52.9	42.3	0.4	4.3	0.0	0.1	100.0
		52.8	44.4	1.1	1.7	0.0	0.0	100.0
		52.8	39.7	0.5	6.1	0.0	0.0	99.1
		52.8	40.7	0.8	5.2	0.0	0.0	99.5
		52.7	42.0	1.4	3.7	0.1	0.0	99.9
		52.6	43.0	1.3	2.3	0.0	0.0	99.3
		52.4	42.3	2.0	2.0	0.0	0.0	98.8
		34.7	29.4	0.0	0.1	33.7	0.0	98.0
		34.7	29.8	0.0	0.0	34.2	0.0	98.7
		34.7	29.1	0.0	0.1	33.5	0.0	97.4
		34.6	29.2	0.0	0.0	33.5	0.0	97.4
		34.6	29.2	0.0	0.0	32.9	0.0	96.7
		34.6	29.3	0.0	0.0	33.7	0.0	97.6
		34.6	28.9	0.0	0.0	33.2	0.0	96.8
3R-1 (3, 8–10)	20.3	52.1	41.7	4.8	0.1	0.0	0.0	98.8
		52.8	40.6	5.5	0.2	0.0	0.1	99.2
		52.4	43.8	1.7	0.5	0.0	0.0	98.5
		41.4	14.0	2.3	39.5	0.0	0.0	97.2
		41.7	14.3	2.4	39.4	0.2	0.0	98.0
		41.8	14.2	2.4	39.3	0.2	0.0	98.0

Table T2 (continued).

Hole, core, section, piece, interval (cm)	Depth (mbsf)	S	Fe	Co	Ni	Cu	Zn	Total
3R-1 (3, 8–10)	20.3	52.5	43.9	0.0	2.2	0.0	0.0	98.6
		52.8	41.3	5.0	0.1	0.0	0.1	99.3
		52.3	44.2	0.0	1.4	0.0	0.0	98.0
		35.2	1.2	0.0	62.4	0.0	0.0	98.8
3R-3 (3, 14–16)	23.3	52.5	45.9	0.0	0.5	0.0	0.0	99.1
		49.6	43.6	0.0	2.0	0.0	0.0	95.4
		52.2	46.1	0.0	0.8	0.0	0.0	99.4
		40.8	19.2	2.6	33.8	0.0	0.0	96.7
		52.0	45.2	0.0	1.3	0.0	0.0	98.6
		51.8	46.5	0.0	0.4	0.0	0.0	99.0
		39.5	19.6	3.3	33.0	0.0	0.0	95.7
		46.5	47.1	0.0	1.2	0.0	0.0	95.2
		34.0	28.6	1.9	32.0	0.0	0.0	96.6
		50.7	45.5	0.0	0.5	0.0	0.0	96.9
		52.1	45.2	0.0	1.4	0.0	0.0	98.9
		50.9	44.0	0.0	3.4	0.0	0.0	98.4
		52.6	45.7	0.0	0.6	0.0	0.0	99.0
		51.0	45.1	0.0	1.1	0.0	0.0	97.3
		50.9	45.6	0.0	0.8	0.0	0.0	97.5
		49.9	45.8	0.0	1.2	0.0	0.0	97.8
		50.7	45.4	0.0	0.1	0.0	0.0	96.7
		50.7	43.7	0.0	0.9	0.0	0.0	96.7
		33.8	25.7	2.3	36.4	0.0	0.0	98.4
8R-2 (4, 23–25)	45.7	39.0	57.4	0.0	1.6	0.0	0.0	98.1
		38.7	57.0	0.0	1.6	0.0	0.0	97.3
		38.7	56.7	0.0	1.4	0.0	0.0	96.8
		47.4	47.4	0.0	1.9	0.0	0.0	96.8
		38.7	56.3	0.0	1.1	0.0	0.0	96.2
		38.6	54.5	0.2	4.6	0.0	0.0	97.9
		52.1	43.8	0.0	2.8	0.0	0.0	98.8
		39.8	57.4	0.0	0.8	0.0	0.0	98.1
		50.2	43.1	0.0	2.4	0.0	0.0	95.7
		51.3	43.6	0.0	2.6	0.0	0.0	97.6
		53.1	45.4	0.0	0.9	0.0	0.0	99.5
		38.8	56.4	0.0	1.2	0.0	0.0	96.4
		38.9	57.3	0.0	1.6	0.0	0.0	97.9
		38.9	56.7	0.0	1.1	0.6	0.0	97.4
		37.8	56.2	0.0	1.4	0.0	0.0	95.4
9R-1 (4, 14–16)	49.2	32.9	29.6	1.6	32.9	0.4	0.0	97.4
		33.1	28.5	1.7	32.5	0.0	0.0	95.8
		33.1	28.5	1.6	32.8	0.1	0.0	96.2
		32.9	28.6	1.5	32.9	0.0	0.0	96.0
12R-3 (7A, 63–65)	66.7	53.0	41.6	4.8	0.5	0.0	0.0	100.0
		53.0	44.2	1.2	1.3	0.0	0.0	99.8
		42.2	13.2	0.6	43.5	0.0	0.0	99.5
		53.2	41.9	0.7	4.0	0.0	0.0	99.9
		35.7	2.6	0.0	62.9	0.0	0.0	101.2
		53.2	40.8	0.6	5.7	0.0	0.0	100.3
		52.9	41.0	5.5	0.9	0.2	0.0	100.4
		53.2	41.6	5.0	0.2	0.0	0.0	100.1
		35.4	1.1	0.0	64.0	0.0	0.0	100.5
		52.1	44.1	0.1	2.3	0.0	0.0	98.6
		34.8	29.6	0.0	0.0	33.7	0.1	98.2
		35.0	30.3	0.0	0.1	34.1	0.0	99.5
		53.0	45.1	0.1	2.2	0.0	0.0	100.5
		35.6	1.9	0.0	64.1	0.0	0.0	101.6
		53.3	41.0	3.7	2.9	0.0	0.0	101.0
		35.6	1.2	0.0	63.3	0.0	0.0	100.1
		53.0	41.9	1.1	4.0	0.0	0.0	100.0
		53.2	40.8	0.3	6.0	0.1	0.0	100.4
		35.5	0.9	0.0	64.3	0.0	0.0	100.7
		35.6	1.8	0.0	63.5	0.0	0.0	100.9
		35.5	1.2	0.0	64.4	0.0	0.0	101.1
		35.5	1.3	0.1	62.7	0.0	0.0	99.6
		52.6	43.8	1.2	1.3	0.0	0.0	98.9
13R-3 (3, 8–11)	71.1	35.3	2.1	0.3	63.0	0.0	0.0	100.6
		35.8	4.1	0.3	62.0	0.0	0.0	102.3

Table T2 (continued).

Hole, core, section, piece, interval (cm)	Depth (mbsf)	S	Fe	Co	Ni	Cu	Zn	Total
13R-3 (3, 8–11)	71.1	35.0	3.5	0.2	61.2	0.0	0.0	100.0
		35.5	3.7	0.1	62.9	0.0	0.0	102.1
		35.5	2.3	0.2	62.9	0.0	0.0	100.8
		53.0	40.0	3.8	3.0	0.0	0.0	99.8
		52.7	41.6	0.1	4.7	0.0	0.0	99.1
		35.5	1.2	0.1	62.8	0.0	0.0	99.5
		35.2	0.8	0.0	63.9	0.0	0.0	99.9
		53.0	40.1	5.7	0.8	0.0	0.0	99.7
		41.3	8.8	1.5	46.8	0.0	0.0	98.6
		52.6	40.4	0.9	5.4	0.0	0.0	99.3
		52.3	43.6	0.6	1.7	0.0	0.0	98.2
		50.4	42.2	1.2	2.1	0.0	0.0	95.9
		53.5	40.4	1.2	5.1	0.0	0.0	100.2
		41.2	8.1	0.5	48.3	0.0	0.0	98.1
		35.3	1.8	0.0	62.8	0.0	0.0	99.8
		51.1	41.4	1.0	3.1	0.0	0.0	96.5
		52.9	39.9	2.7	3.7	0.0	0.0	99.1
		35.4	1.9	0.1	63.2	0.0	0.0	100.6
		52.8	38.7	1.6	6.1	0.0	0.0	99.3
		52.0	41.1	1.2	3.1	0.1	0.0	97.5
		52.7	36.6	1.0	8.7	0.0	0.0	99.0
		52.7	41.2	4.4	0.9	0.0	0.0	99.3
		52.9	41.5	0.4	4.4	0.0	0.0	99.1
		42.9	14.7	2.3	38.1	0.0	0.0	98.1
		35.6	0.7	0.0	63.2	0.0	0.0	99.5
		51.8	42.5	1.4	2.0	0.0	0.0	97.7
		52.9	40.2	1.3	4.7	0.0	0.0	99.1
		51.8	40.3	4.8	0.7	0.0	0.0	97.7
14R-1 (7A, 34–36)	73.1	33.1	27.4	2.1	33.8	0.0	0.0	96.4
		39.4	55.7	0.0	2.2	0.0	0.0	97.4
		36.8	45.3	0.9	14.0	0.1	0.0	97.0
		33.3	29.9	1.9	31.5	0.0	0.0	96.7
		38.7	55.1	0.1	2.5	0.0	0.0	96.3
		32.9	27.8	2.1	34.9	0.0	0.0	97.8
		39.4	56.4	0.1	2.5	0.0	0.0	98.3
		32.6	27.6	2.1	34.4	0.0	0.0	96.8
		39.3	56.3	0.1	2.4	0.0	0.0	98.1
		39.0	55.4	0.1	2.4	0.0	0.0	96.9
		32.3	27.0	2.1	34.2	0.0	0.0	95.6
		33.2	27.8	2.2	35.2	0.0	0.0	98.4
		39.4	55.7	0.1	2.4	0.0	0.0	97.6
		34.9	29.6	0.0	0.0	32.8	0.0	97.4
		34.9	29.5	0.0	0.0	32.7	0.0	97.1
		39.2	56.3	0.1	2.6	0.0	0.0	98.2
		33.5	28.1	2.2	35.9	0.0	0.0	99.7
		39.1	56.1	0.0	2.5	0.0	0.0	97.8
		38.8	54.3	0.1	3.9	0.0	0.0	97.2
		39.3	56.4	0.1	2.4	0.0	0.0	98.2
		39.7	56.5	0.1	2.5	0.0	0.0	98.8
		33.6	7.9	0.0	0.1	0.1	57.7	99.4
		39.4	56.5	0.1	2.5	0.0	0.0	98.4
		33.1	28.5	2.1	35.3	0.0	0.1	99.1
		39.4	56.9	0.0	2.5	0.0	0.0	98.8
		33.6	8.8	0.0	0.1	0.1	56.9	99.4
		33.7	8.1	0.0	0.0	0.1	57.4	99.3
		33.3	7.2	0.0	0.0	0.0	56.9	97.4
		38.4	55.7	0.0	2.3	0.0	0.1	96.5
		39.2	56.2	0.0	2.4	0.0	0.0	97.9
		33.6	28.7	2.1	34.8	0.0	0.0	99.2
		33.5	7.3	0.0	0.1	0.0	58.0	99.0
		39.6	56.6	0.1	2.3	0.0	0.1	98.7
		39.8	56.4	0.1	2.4	0.0	0.2	98.9
		32.8	28.1	2.4	34.2	0.0	0.0	97.5
		39.6	57.1	0.1	1.7	0.0	0.1	98.6
		32.8	27.6	2.2	35.0	0.0	0.0	97.6
		39.6	56.7	0.0	2.5	0.0	0.0	98.9
		39.2	55.8	0.1	2.4	0.0	0.0	97.5
		39.4	56.3	0.1	2.3	0.0	0.0	98.2
		39.5	56.5	0.1	2.3	0.0	0.0	98.5

Table T2 (continued).

Hole, core, section, piece, interval (cm)	Depth (mbsf)	S	Fe	Co	Ni	Cu	Zn	Total
14R-1 (7A, 34–36)	73.1	39.6	57.4	0.1	1.9	0.0	0.0	99.0
		39.5	56.9	0.0	2.0	0.0	0.0	98.4
		39.6	57.0	0.0	2.0	0.0	0.0	98.6
		34.6	29.5	0.0	0.0	32.6	0.2	96.9
		39.6	56.2	0.1	2.2	0.2	0.0	98.3
		39.4	55.8	0.0	2.2	0.0	0.0	97.5
		33.8	10.6	0.1	0.0	0.0	54.5	99.1
		39.5	56.6	0.1	2.3	0.0	0.4	98.9
		34.9	30.2	0.0	0.0	33.1	0.1	98.3
		34.8	29.6	0.0	0.0	33.0	0.1	97.4
		34.9	29.9	0.0	0.0	32.9	0.2	98.0
		34.8	29.1	0.0	0.1	32.3	0.1	96.5
		32.9	25.8	2.0	34.8	1.1	0.0	96.6
		33.4	5.8	0.0	0.0	0.0	59.2	98.5
		39.5	56.4	0.1	2.5	0.0	0.2	98.6
		33.5	9.4	0.0	0.1	1.3	55.0	99.4
15R-3 (1, 15–17)	80.6	39.4	56.1	0.1	3.1	0.0	0.0	98.8
		34.7	30.4	0.0	0.1	33.0	0.0	98.1
		39.3	56.7	0.1	2.6	0.0	0.0	98.8
		39.4	56.3	0.1	3.1	0.0	0.0	99.0
		39.1	54.2	0.1	4.1	0.0	0.0	97.6
		39.2	54.2	0.1	4.1	0.0	0.0	97.7
		39.2	54.8	0.1	4.1	0.0	0.0	98.2
		40.4	55.3	0.0	2.5	0.0	0.0	98.2
		52.6	46.1	0.0	0.3	0.3	0.0	99.3
		34.8	29.5	0.0	0.2	33.1	0.0	97.6
		40.8	24.2	0.8	30.2	0.2	0.0	96.2
		34.7	29.5	0.0	0.3	32.4	0.0	96.9
		42.1	24.8	0.7	30.2	0.0	0.0	97.8
		40.2	54.0	0.1	1.9	2.4	0.0	98.5
		39.2	55.4	0.1	3.4	0.0	0.0	98.1
		39.4	55.1	0.1	3.4	0.0	0.0	98.0
		34.7	30.3	0.0	0.1	32.7	0.1	97.8
		39.5	55.9	0.1	3.4	0.0	0.0	98.9
		34.7	30.2	0.0	0.0	33.5	0.1	98.5
		40.6	55.6	0.1	1.3	0.0	0.0	97.6
		40.6	56.3	0.1	0.9	0.0	0.0	97.9
		34.3	31.6	0.0	0.1	30.3	0.0	96.4
		40.1	56.0	0.1	1.2	0.0	0.0	97.5
19R-2 (209, 34–36)	98.7	53.1	38.3	9.0	0.1	0.0	0.0	100.6
		39.8	52.7	0.1	3.3	0.0	0.0	95.9
		38.5	51.3	0.0	4.1	0.0	0.0	94.0
		51.9	44.5	0.2	2.2	0.0	0.0	98.8
		40.4	50.3	0.2	6.0	0.0	0.0	96.9
		40.8	53.1	0.1	4.2	0.0	0.0	98.3
		52.6	38.8	7.8	0.3	0.0	0.0	99.6
		53.1	39.3	8.6	0.2	0.0	0.0	101.2
		52.3	36.5	9.3	0.5	0.0	0.0	98.6
		41.0	55.2	0.1	2.5	0.0	0.0	98.8
		40.2	54.5	0.1	3.0	0.0	0.0	97.9
		41.0	25.8	0.8	29.1	0.0	0.0	96.6
		39.6	54.0	0.1	4.5	0.1	0.0	98.3
		49.2	39.5	9.1	0.4	0.0	0.0	98.3
		39.4	53.6	0.2	5.7	0.0	0.1	99.0
		53.2	40.5	6.0	0.4	0.0	0.0	100.2
		38.9	53.2	0.2	5.7	0.0	0.0	98.0
		39.4	53.4	0.2	5.7	0.0	0.0	98.7
		40.5	54.9	0.2	2.7	0.0	0.0	98.4
		52.6	37.3	8.9	0.5	0.0	0.0	99.4
		38.3	52.2	0.2	5.5	0.0	0.0	96.2
		33.3	26.3	1.9	36.8	0.0	0.0	98.2
		40.6	54.5	0.2	2.7	0.0	0.0	98.0
		39.0	54.0	0.2	4.5	0.0	0.0	97.8
		39.5	53.3	0.2	5.3	0.0	0.1	98.4
		39.0	53.8	0.1	4.9	0.0	0.1	97.9
20R-3 (13, 83–85)	105.3	35.2	30.0	0.0	0.0	34.1	0.0	99.3
		34.9	29.8	0.0	0.0	34.2	0.0	98.9
		34.9	30.1	0.0	0.0	34.5	0.0	99.5

Table T2 (continued).

Hole, core, section, piece, interval (cm)	Depth (mbsf)	S	Fe	Co	Ni	Cu	Zn	Total
20R-3 (13, 83–85)	105.3	34.5	29.6	0.0	0.0	34.1	0.0	98.3
		34.7	29.9	0.0	0.0	34.2	0.0	98.8
		34.8	29.7	0.0	0.0	34.2	0.0	98.7
		34.8	30.0	0.0	0.0	34.3	0.0	99.1
23R-3 (1, 6–8)	119.0	33.2	32.8	1.4	31.2	0.0	0.1	98.7
		33.3	32.8	1.4	31.4	0.0	0.0	98.9
		34.2	29.7	0.6	8.0	26.2	0.1	98.8
		33.4	32.1	1.4	31.4	0.0	0.0	98.4
		33.1	30.7	1.5	31.3	0.0	0.0	96.6
		33.1	32.4	1.4	31.1	0.0	0.0	98.0
		34.8	29.3	0.0	0.0	33.1	0.1	97.4
		33.9	29.1	0.0	0.0	33.2	0.3	96.5
		33.4	31.7	1.5	31.6	0.2	0.0	98.3
		33.1	30.6	1.4	31.5	0.0	0.0	96.5
		34.7	28.8	0.0	0.1	32.8	0.1	96.4
		32.8	30.9	1.5	32.2	0.1	0.0	97.5
		34.7	29.3	0.0	0.0	33.0	0.2	97.2
		34.6	31.1	0.2	0.6	29.1	0.8	96.4
		33.1	31.9	1.5	32.2	0.0	0.0	98.6
		34.9	30.7	0.0	0.3	31.9	0.4	98.2
		34.8	29.5	0.0	0.0	33.3	0.1	97.7
		33.4	33.3	1.5	31.4	0.0	0.0	99.6
		33.3	32.2	1.5	32.4	0.0	0.0	99.4
		34.9	29.3	0.0	0.0	33.3	0.3	97.7
		32.7	30.2	1.4	31.8	0.0	0.0	96.1
		32.4	30.6	1.4	32.1	0.0	0.0	96.6
		34.8	29.1	0.0	0.0	33.3	0.2	97.4
		34.7	29.2	0.0	0.0	33.1	0.3	97.4
		34.0	28.8	0.0	0.0	31.6	0.4	94.9
		34.8	29.2	0.0	0.1	33.2	0.3	97.6
		33.3	32.8	1.5	31.6	0.2	0.0	99.3
		33.3	33.0	1.5	30.6	0.9	0.0	99.3
		33.2	31.7	1.6	32.1	0.1	0.0	98.8
		34.8	29.5	0.0	0.1	32.9	0.2	97.5
		34.8	29.4	0.0	0.0	33.3	0.2	97.6
		34.8	28.9	0.0	0.0	33.2	0.1	97.0
		34.8	29.1	0.0	0.0	33.2	0.2	97.3
		34.2	29.1	0.0	0.0	32.6	0.1	95.9
		33.2	32.5	1.5	32.0	0.0	0.0	99.2
		33.3	32.7	1.4	31.0	0.0	0.0	98.5
		34.8	29.1	0.0	0.0	33.3	0.3	97.5
		35.0	29.1	0.0	0.0	33.3	0.2	97.5
		34.6	29.1	0.0	0.0	33.0	0.4	97.2
24R-1 (10, 78–80)	121.6	33.3	31.0	1.3	32.5	0.0	0.0	98.2
		34.4	29.3	0.0	0.1	32.9	0.5	97.1
		52.7	45.9	0.0	0.4	0.0	0.0	99.1
		52.9	45.8	0.0	0.2	0.0	0.0	99.0
		52.4	46.2	0.0	0.6	0.0	0.0	99.3
		52.2	45.4	0.0	0.7	0.0	0.0	98.3
		41.5	23.0	2.3	30.7	0.2	0.1	97.7
		41.9	22.2	2.2	31.3	0.4	0.0	98.0
		34.5	30.5	0.0	0.1	33.2	0.4	98.6
		51.7	45.8	0.0	0.0	0.0	0.0	97.6
		41.3	23.6	2.1	28.8	0.1	0.0	96.0
		34.9	29.7	0.0	0.0	33.7	0.3	98.7
		52.7	45.8	0.0	0.9	0.0	0.0	99.5
		51.7	46.2	0.0	0.8	0.3	0.0	99.0
		35.0	29.5	0.0	0.0	33.3	0.4	98.2
24R-2 (9, 101–103)	123.1	39.3	58.3	0.0	0.2	0.0	0.0	97.8
		39.7	58.7	0.0	0.4	0.0	0.0	98.8
		35.9	23.7	1.5	34.6	0.0	0.0	95.7
		35.0	25.9	1.6	34.4	0.0	0.0	97.0
		33.0	23.2	1.9	32.5	0.3	0.0	90.9
		39.6	58.1	0.0	0.7	0.0	0.0	98.4
		37.0	24.5	1.7	32.6	0.0	0.0	95.8
		35.9	23.2	1.6	35.4	0.0	0.0	96.1
		33.3	25.4	1.4	35.5	0.0	0.0	95.5
		32.8	25.5	1.6	35.4	0.0	0.0	95.3

Table T2 (continued).

Hole, core, section, piece, interval (cm)	Depth (mbsf)	S	Fe	Co	Ni	Cu	Zn	Total
24R-2 (9, 101–103)	123.1	33.3	28.0	1.6	34.7	0.0	0.0	97.5
		33.1	27.5	1.9	35.9	0.0	0.0	98.3
		33.2	28.5	1.7	34.9	0.1	0.0	98.5
		33.2	28.2	1.7	34.7	0.0	0.0	97.8
		33.3	27.1	1.8	36.3	0.0	0.0	98.5
		33.5	31.6	1.6	31.8	0.0	0.1	98.4
		33.4	32.4	1.8	32.1	0.0	0.1	99.8
		33.3	31.4	1.6	32.5	0.0	0.0	98.8